

Original Article

Cite this article: Kenny GG, O'Sullivan GJ, Alexander S, Simms MJ, Chew DM, and Kamber BS (2019) On the track of a Scottish impact structure: a detrital zircon and apatite provenance study of the Stac Fada Member and wider Stoer Group, NW Scotland. *Geological Magazine* **156**: 1863–1876. <https://doi.org/10.1017/S0016756819000220>

Received: 11 October 2018

Revised: 28 February 2019

Accepted: 2 March 2019


First published online: 24 April 2019

Keywords:

Stac Fada Member; impact structure; zircon; apatite; provenance

Author for correspondence: Gavin G. Kenny, Email: gkenny@trinity.dublincityu.ie

On the track of a Scottish impact structure: a detrital zircon and apatite provenance study of the Stac Fada Member and wider Stoer Group, NW Scotland

Gavin G. Kenny^{1,2,*} , Gary J. O'Sullivan¹, Stephen Alexander¹, Michael J. Simms³, David M. Chew¹ and Balz S. Kamber^{1,4}

¹Department of Geology, School of Natural Sciences, Trinity College Dublin, Dublin 2, Ireland; ²Department of Geosciences, Swedish Museum of Natural History, SE-104 05 Stockholm, Sweden; ³Department of Natural Sciences, National Museums Northern Ireland, Cultra, BT18 0EU Northern Ireland, UK and ⁴School of Earth, Environmental and Biological Sciences, Queensland University of Technology, GPO Box 2434, Brisbane, QLD 4001, Australia

Abstract

The Stac Fada Member of the Stoer Group, within the Torridonian succession of NW Scotland, is a melt-rich, impact-related deposit that has not been conclusively correlated with any known impact structure. However, a gravity low approximately 50 km east of the preserved Stac Fada Member outcrops has recently been proposed as the associated impact site. We investigate the location of the impact structure through a provenance study of detrital zircon and apatite in five samples from the Stoer Group. Our zircon U–Pb data are dominated by Archaean grains (> 2.5 Ga), consistent with earlier interpretations that the detritus was largely derived from local Lewisian Gneiss Complex, whereas the apatite data (the first for the Stoer Group) display a single major peak at *c.* 1.7 Ga, consistent with regional Laxfordian metamorphism. The almost complete absence of Archaean-aged apatite is best explained by later heating of the > 2.5 Ga Lewisian basement (the likely source region) above the closure temperature of the apatite U–Pb system (*c.* 375–450°C). The U–Pb age distributions for zircon and apatite show no significant variation with stratigraphic height. This may be interpreted as evidence that there was no major change in provenance during the course of deposition of the Stoer Group or, if there was any significant change, the different source regions were characterized by similar apatite and zircon U–Pb age populations. Consequently, the new data do not provide independent constraints on the location of the structure associated with the Stac Fada Member impact event.

1. Introduction

The geological record of Britain and Ireland describes a rich history of events spanning almost 3 Gyr but no unequivocal impact structures have yet been identified. Evidence for impact events has been proposed at three stratigraphic levels: the Mesoproterozoic Stac Fada Member impact ejecta unit in the Stoer Group, northwestern Scotland (Amor *et al.* 2008), which contains, for example, the high-pressure polymorph of zircon, reidite (Reddy *et al.* 2015); a deposit of reworked microtektites in the Triassic Mercia Mudstone Group of southwestern England, from which multiple orientations of planar deformation features (PDFs) in shocked quartz have been documented and measured (Walkden *et al.* 2002; Kirkham, 2003); and a purported Palaeogene impact ejecta layer on the Isle of Skye, Scotland (Drake *et al.* 2017) that awaits confirmation with unequivocal documentation of shock features. Only the microtektite-bearing Triassic deposit has been linked to a known impact structure – the approximately 100 km diameter Manicouagan impact structure, Quebec, Canada (Thackrey *et al.* 2009). The impact structure associated with the Stac Fada Member has yet to be identified, but various lines of evidence have been used to suggest possible source locations for the material, even prior to its recognition as being related to an impact. These include sedimentary features, thickness variations and an anisotropy of magnetic susceptibility study (Lawson, 1972; Stewart, 2002; Young, 2002; Amor *et al.* 2008, 2011; Simms, 2015). Most recently, Simms (2015) proposed that a geophysical anomaly known as the Lairg Gravity Low, which has a diameter of about 40 km and is centred approximately 50 km east of the Stac Fada Member outcrops, may indicate the location of the now-buried structure. Despite a lack of consensus on the likely location or size of the impact structure associated with the Stac Fada Member, it presently represents the best prospect for the first identification of an impact structure in Britain or Ireland. In this context, we report the results of a detrital zircon and apatite U–Pb provenance study of sedimentary rocks of the Stac Fada Member and wider Stoer Group with the aim of testing whether there was a change

© The Author(s), 2019. Published by Cambridge University Press. This is an Open Access article, distributed under the terms of the Creative Commons Attribution licence (<http://creativecommons.org/licenses/by/4.0/>), which permits unrestricted re-use, distribution, and reproduction in any medium, provided the original work is properly cited.

CAMBRIDGE
UNIVERSITY PRESS

in sediment source contemporaneous with the impact that might yield information on the possible location of the impact structure.

2. Study setting

2.a. Regional setting

The Stac Fada Member occurs within the Stoer Group, an approximately 2 km thick sequence that is the oldest of three groups of alluvial, lacustrine and aeolian sediments (Stoer, Sleat and Torridon groups) that are collectively termed the ‘Torridonian.’ During the late Mesoproterozoic and early Neoproterozoic eras, the Torridonian was deposited on the edge of the Laurentian Shield, near the approximately contemporaneous Grenville orogenic belt (Stewart, 2002). The sedimentary succession was deposited unconformably upon the high-grade metamorphic basement of the Lewisian Gneiss Complex. The Lewisian is composed of a number of Archaean terranes with differing protolith ages, which have experienced a range of metamorphic events. The polyphase metamorphic history is reflected in the complex pattern of Lewisian zircon U–Pb ages distributed along the concordia between *c.* 3.0 Ga and the time of granulite facies metamorphism at *c.* 2.5 Ga (Whitehouse & Kemp, 2010). Some zircon grains also record older Archaean events in the form of inherited cores dated to *c.* 3.1 Ga and *c.* 3.5 Ga (Kinny & Friend, 1997). The Proterozoic history of the Lewisian is dominated by *c.* 1.9 Ga felsic igneous activity in a magmatic arc setting, for example, the South Harris Complex of the Outer Hebrides (e.g. Whitehouse & Bridgwater, 2001; Mason *et al.* 2004), the Ben Stack granites near Loch Laxford, north of Stoer (Goodenough *et al.* 2013), and the Ard gneiss in the Gairloch area, south of Gruinard Bay (Park *et al.* 2001). The final assembly of various terranes composing the Lewisian is recorded by *c.* 1.7 Ga Laxfordian metamorphism (e.g. Heaman & Tarney, 1989; Waters *et al.* 1990; Corfu *et al.* 1994; Kinny & Friend, 1997; Zhu *et al.* 1997; Love *et al.* 2010). However, zircon of this age is relatively rare and mainly found in pegmatites (Park *et al.* 2001). Detrital zircon grains in sedimentary rocks of the Stoer Group have reported ages corresponding to those known from the Lewisian (Rainbird *et al.* 2001; Kinnaird *et al.* 2007). This is consistent with the original interpretation that detritus in the Stoer Group was primarily sourced from the Lewisian (e.g. Stewart, 1982, 1990, 2002; Van de Kamp & Leake, 1997). Later deformation in the region included the thrusting of younger Moine metamorphic rocks westwards over the unmetamorphosed Torridonian during the Caledonian Orogeny. However, the Torridonian escaped significant deformation, and today the Stac Fada Member crops out approximately 20 km west of the Moine Thrust Zone (Fig. 1).

2.b. The Stac Fada Member

The Stac Fada Member, which is usually *c.* 10 m thick and can be traced along-strike for more than 50 km (Fig. 1), has a distinctive appearance with fragments of dark green, vesicular, devitrified glass accompanying mudstone, sandstone and gneiss clasts up to 0.5 m across in a poorly sorted sand matrix (Stewart, 2002). Sandstone rafts reach 15 m in length at the type locality of the unit at Stac Fada, near the village of Stoer (Stewart, 2002). The Stac Fada Member was previously interpreted as a mudflow, or series of mudflows, related to endogenic volcanic processes (e.g. Lawson, 1972; Sanders & Johnston, 1989; Stewart, 1990; Young, 2002), but the identification of PDFs in quartz led to its reinterpretation as an ejecta deposit associated with a bolide impact (Amor *et al.*

2008). Arguably the best evidence that the deposition of the Stac Fada Member was related to a hypervelocity impact is the presence of shock-metamorphosed zircon with lamellae of the high-pressure ZrSiO₄ polymorph, reidite (Reddy *et al.* 2015).

Following its reinterpretation as an impact-related deposit, the Stac Fada Member has been divided into three distinct units at the Enard Bay section (Branney & Brown, 2011). The lowermost stratigraphy, which varies in thickness from 4 to 10 m, comprises a massive suevite with matrix-supported devitrified melt fragments as well as gneiss and mudstone clasts. This grades into a similar unit, distinguished by its abundant matrix-supported whole and broken accretionary lapilli up to 15 mm in diameter and the onset of stratification near its top. The uppermost portion of the Stac Fada Member comprises a thin (≤ 3 cm) layer of clast-supported dust pellets (aggregates of ash which lack the distinct internal structure of accretionary lapilli) < 5 mm in diameter. The two lower units are interpreted to have formed from a decelerating granular density current that rapidly waxed and then waned, whereas the thin layer of pellets is interpreted to represent direct fallout from a residual atmospheric dust plume (Branney & Brown, 2011).

2.c. Locating the impact site

Various lines of evidence have been put forward in attempts to constrain the location and proximity of the source material for the Stac Fada Member, but there is no current consensus. The most pertinent points are noted below.

Upon interpreting the Stac Fada Member as an impact-related unit, Amor *et al.* (2008) suggested that the relatively thick and distinctively continuous nature of the unit over tens of kilometres is indicative of quite a proximal source location, although no distance was specified. However, the lack of seismites or any significant soft-sediment deformation in the underlying succession has been interpreted as suggesting that the impact structure was still a significant distance away, ‘perhaps tens of kilometres’ (Simms, 2015, p. 755).

Variations in thickness and lithology along the effectively linear outcrop trace of the Stac Fada Member (Fig. 1) have been cited as indicative of proximal-distal changes. The greater thickness of the deposit in the more northerly outcrops (*c.* 10–15 m thick at Stoer and Enard Bay compared with 4–6 m thick further south; Simms, 2015) has been interpreted as tentative evidence that the southern sites may be more distal to the impact (Amor *et al.* 2008; Simms, 2015). The abundance of accretionary lapilli in the Stac Fada Member at Enard Bay (and their absence further south) has also been proposed as evidence that this is the most proximal presently exposed outcrop (e.g. Simms, 2015).

The Stac Fada Member is largely massive and was emplaced without significant erosion of underlying material. This means that there is a paucity of sedimentary structures that could indicate the direction from which it was deposited. Wedge-shaped intrusions of melt-bearing breccia into the strata beneath the Stac Fada Member have been regarded as among the few potential indicators, but different authors have interpreted them as indicating different directions of movement. Lawson (1972), working before the unit was recognized as an impact-related deposit, and Amor *et al.* (2008) proposed that material was moving from west to east, leading Amor *et al.* (2008) to suggest that the impact structure may be offshore beneath the Minch Basin. Conversely, Stewart (2002) interpreted the same folds and upturned beds as indicating movement from east to west. Sanders & Johnston (1989, figs 2, 3)

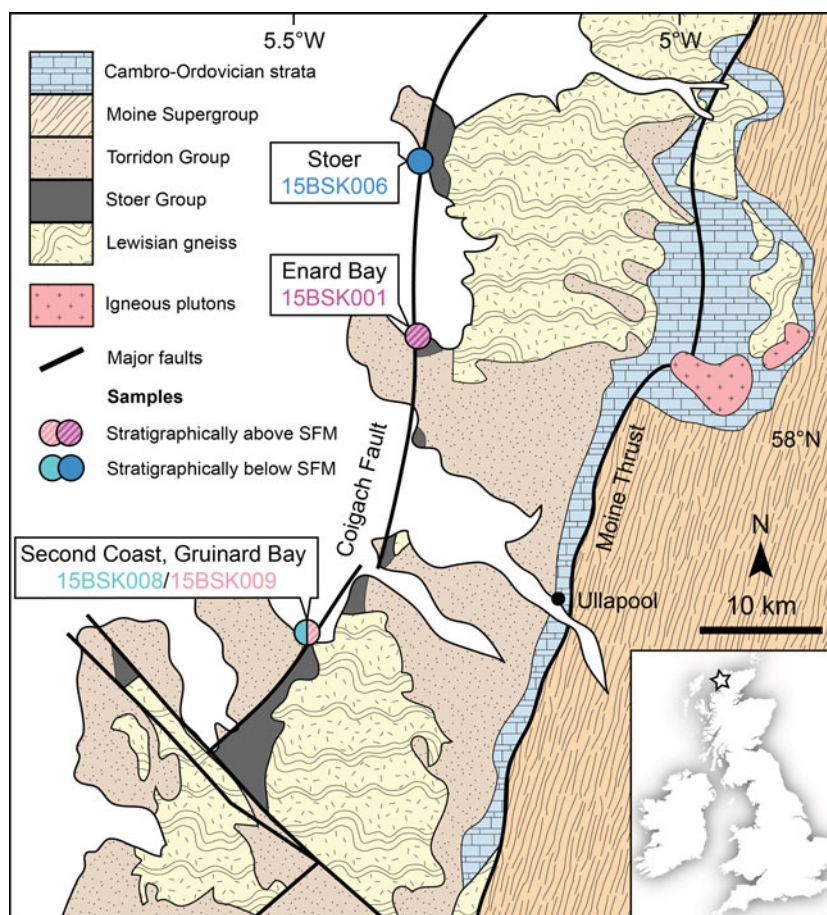


Fig. 1. (Colour online) Regional geology of NW Scotland with sample locations for this study. Map modified from Simms (2015). Note that the Torridonian comprises the Stoer and Torridon groups, as well as the Sleat Group which is exposed south of this area. Sample 15BSK_X_SFM is a combination of rocks from the Stac Fada Member (SFM) at all three localities. The Minch basin, proposed as a possible location of the Stac Fada Member-related impact structure by Amor *et al.* (2008), lies offshore (i.e. where the legend is situated on the map), whereas the centre of the Lairg gravity low, suggested as a possible impact site by Simms (2015), lies approximately 30 km east of the Moine Thrust.

described the wedge-shaped geometry of the base of the Stac Fada Member at Stoer and documented thinning to the north and west. Young (2002) interpreted small-scale asymmetrical folds and flame structures in sandstones within the Stac Fada Member as evidence for movement of material from two opposing directions, one from the SSW and the other from the NNE.

With the recognition that the Stac Fada Member was impact-derived (Amor *et al.* 2008), it follows that the deposit must originate from a single location. Simms (2015) suggested that the directional variability reported by Young (2002) may be due to rotation of the sandstone rafts during transportation, an interpretation supported by the apparently random palaeomagnetic orientations of the rafts (Irving & Runcorn, 1957; Stewart, 2002). Most recently, Simms (2015, fig. 5) has interpreted the wedge-shaped intrusions of melt-bearing breccia into the strata beneath the Stac Fada Member as evidence for emplacement from a source to the east and argued that because the oversteepened sandstone beds above the intrusive wedges are anchored into the pre-impact stratigraphy they preserve a more robust record of the emplacement direction of the ejecta.

Other sedimentary features that may indicate transport directions have been documented at Enard Bay. These include planar cross-beds and lapilli long axes in the upper part of the Stac Fada Member, as well as gently plunging troughs subsequently incised into the lapilli beds. Simms (2015) interpreted all of these

features to indicate that material was broadly moving from east to west during deposition. Further south, Simms (2015) documented curved fractures on the upper surface of the Stac Fada Member and suggested that these may be related to the transport direction, with their convex-westwards configuration indicating the direction of flow. Similarly, if the concave-up surfaces documented by Simms (2015) within the Stac Fada Member can be interpreted as thrust planes within a viscous flow, they would also be consistent with movement from the east.

In a non-peer-reviewed abstract, Amor *et al.* (2011) reported the results of an anisotropy of magnetic susceptibility study of the Stac Fada Member that supported an impact structure lying to the west of the present Stac Fada Member outcrops.

In light of the varying interpretations of the evidence within the Stac Fada Member itself, the overlying succession has also been studied with the aim of elucidating a possible source location for the impact ejecta material. The Stac Fada Member is succeeded by up to 100 m of lacustrine, plane-bedded sedimentary rocks (the Poll à Mhuil Member; Fig. 2) at all but the most southerly sites (Stewart, 2002; Simms, 2015) before fluvial and aeolian deposition commences in the Meall Dearg Formation. These two lithostratigraphic units provide evidence of a dramatic reconfiguration of the regional drainage pattern following deposition of the Stac Fada Member (Stewart, 2002). The Poll à Mhuil Member was interpreted as a post-impact lake by Amor *et al.* (2008). Ripple

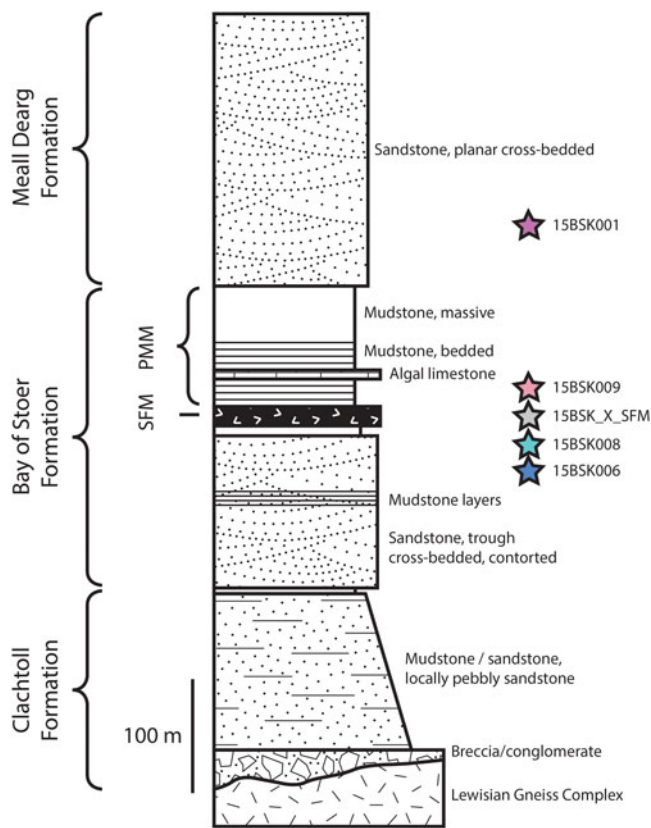


Fig. 2. (Colour online) Generalized stratigraphic column for the Stoer Group at Stoer. Modified from Goodenough & Krabbendam (2011, fig. 32). Note that only sample 15BSK006 was taken at this locality and the stratigraphic location of the other samples are indicative on a relative time basis. There is significant lateral lithology variation within the Stoer Group (Stewart, 2002). PMM – Poll à Mhuil Member; SFM – Stac Fada Member.

cross-lamination (Stewart, 2002) and cross-bedding (Simms, 2015) indicate that flow into the lakes was broadly from the west, suggesting that eastwards-flowing rivers were dammed by debris located east of the present outcrops (Simms, 2015).

In contrast to the variable palaeocurrent azimuths of the pre-Stac Fada Member succession, fluvial sediments in the Meall Dearg Formation consistently record flow to the west (Stewart, 2002; Simms, 2015; Lebeau & Ielpi, 2017) but with evidence for a broadly radial drainage configuration centred on a focal point to the east (Simms, 2015, fig. 6). Stewart (2002) had interpreted this palaeoflow configuration as related to tectonic uplift on the eastern flank of the basin but, in light of the impact evidence, Simms (2015) reinterpreted the apparently radial drainage system of the Meall Dearg Formation as a consequence of post-impact regional doming.

Geophysical data can play a key role in the study of impact structures once unambiguous evidence for an impact has already been documented (such as the identification of shatter cones, PDFs in quartz, or shock microtwins or reidite in zircon). This is particularly relevant to structures that are not, or are only partially, exposed at the Earth's surface (e.g. the Chicxulub structure buried on the Yucatán Peninsula, Mexico; Hildebrand *et al.* 1998). A common geophysical anomaly associated with impact structures is a broadly concentric gravity low which in larger structures (diameter > 30 km) is likely to contain a central gravity high (Grieve & Pilkington, 1996; Morgan & Rebolledo-Vieyra, 2013). Simms (2015) proposed that a significant gravity low centred near

the village of Lairg in northern Scotland, approximately 50 km east of the Stac Fada Member outcrops, may represent the impact structure from which the Stac Fada Member material was derived, which is consistent with his interpretation of directional data from the Stac Fada Member and the overlying succession. Previous interpretations have ascribed this gravity low to a Caledonian granite pluton, an Archaean granite in the basement, a buried wedge of Torridonian sedimentary rocks and/or a region of thickened Moine Supergroup rocks (see discussion in Leslie *et al.* 2010). Arguably the most plausible explanation for the gravity low was offered by Leslie *et al.* (2010), who ascribed it to a package of Moine rocks of 5–6 km thickness on the basis of detailed mapping and modelling. There is also a conspicuous gravity low to the west of the Stac Fada Member outcrops in the Minch Basin, which was proposed as the impact site by Amor *et al.* (2008, 2011). However, the thick post-Palaeozoic sediment fill there (Binns *et al.* 1975) provides the most plausible explanation of this feature.

Despite the numerous lines of investigation there is no consensus on the location of the impact structure associated with the Stac Fada Member.

3. A new approach

We investigate the possible location of the impact structure through a detrital zircon and apatite U–Pb provenance investigation of five samples from below, within and above the impact-related unit (Fig. 2). Zircon is a physically and chemically robust mineral that is readily dateable by the U–Pb method and is almost ubiquitous in clastic sediments; it is a well-established and powerful tool in provenance studies (e.g. Thomas, 2011). Recent advances in U–Pb dating of common Pb-bearing minerals (e.g. Chew *et al.* 2011, 2014; Thomson *et al.* 2012) mean that it is now possible to complement detrital zircon analyses with data from other U-bearing heavy minerals. The utility of including apatite in detrital studies (e.g. O'Sullivan *et al.* 2016) stems from the fact that it crystallizes in significant volumes in a much wider range of igneous rock types than zircon (as a result of the limited ability of rock-forming minerals to accept into their structure the amount of phosphorus that occurs in most rocks; Piccoli & Candela, 2002) and, unlike zircon, it crystallizes in significant volumes in metamorphic rocks of all grades and most protolith types (Spear & Pyle, 2002). Secondly, apatite is more likely than zircon to represent first-cycle detritus as it is prone to dissolution at source by acidic meteoric and pedogenic waters (Morton & Hallsworth, 1999). Despite being prone to dissolution at source (Joosu *et al.* 2016) apatite is found in non-trivial abundance in nearly all Quaternary sediments (Nechaev & Ispording, 1993) and, because it is stable during diagenesis (due to the liberation of organic P and P adsorbed onto the surface of clay minerals; e.g. Bouch *et al.* 2002), the detrital apatite signal is likely to be preserved once buried. These factors result in detrital apatite U–Pb data (i) being able to record events such as magma-poor orogenesis that are not well represented in the detrital zircon record (O'Sullivan *et al.* 2016), and (ii) having a greater likelihood of recording relatively recent tectonic events than the detrital zircon U–Pb system, which is more likely to be dominated by plentiful polycyclic detritus. It is important to note that although apatite can record events not visible in the zircon record, a single geological event can often produce contrasting zircon and apatite age distributions; this is because the lower closure temperature of the U–Pb system in apatite (c. 375–450°C) compared with that of zircon (> 900°C) means that the former may record prolonged cooling. Inversely,

the disparity of the U–Pb closure temperatures of the two minerals means that a relatively low-temperature event may reset apatite U–Pb ages without affecting the zircon ages in the same rock.

Although the Stoer Group has previously been studied in terms of detrital zircon U–Pb analysis (Rainbird *et al.* 2001; Kinnaird *et al.* 2007), we build on this work with a high-analysis-number, coupled zircon and apatite U–Pb study. Our specific aims are to understand: (i) whether there are new U–Pb age populations in the succession overlying the impact-related unit that might reflect the presence of previously unexposed rocks brought to the Earth's surface by the impact event; (ii) whether there is an absence of any specific U–Pb age populations in the lacustrine sediments (Poll à Mhuilt Member) above the Stac Fada Member, which may reflect specific source terrain(s) being cut-off as a consequence of impact-related drainage reconfiguration; (iii) whether there is any discernible difference between the heavy mineral assemblages of the fluvial sediments underlying the Stac Fada Member (which were sourced from multiple directions) and those of the fluvial sediments above the Stac Fada Member (which were sourced solely from the east), and whether this might indicate a possible location of the impact structure; and (iv) whether detrital apatite in the Stoer Group records different ages and events compared with detrital zircon, and if the former might have additional utility for recording stratigraphic changes through its ability to highlight a wide range of events and/or its increased likelihood of representing first-cycle detritus.

4. Materials and methods

4.a. Samples

Five samples were processed for zircon and apatite U–Pb analysis. Two were collected from stratigraphically beneath the Stac Fada Member, one from the Stac Fada Member itself, and two from stratigraphically above the impact-related layer (Fig. 2). The samples are listed below in stratigraphic order from lowest to highest, relative to the Stac Fada Member.

Sample 15BSK006 (Stoer; 58.20134° N, 5.34757° W; Fig. 1) is a well-bedded sandstone from the pre-impact fluvial succession. It was sampled approximately 10 m stratigraphically below the base of the Stac Fada Member at the Bay of Stoer in what is mapped as undivided Bay of Stoer Formation (British Geological Survey, 2002).

Sample 15BSK008 (Second Coast, Gruinard Bay; 57.86136° N, 5.49697° W) is a sandstone similar to sample 15BSK006 and was collected immediately below the Stac Fada Member, where the sediment was disturbed by ballistically emplaced boulders of country rocks.

Sample 15BSK_X_SFM is composed of green, devitrified glass-bearing Stac Fada Member material from all three sample sites (Fig. 1). Collection from the Stac Fada Member was primarily focused on obtaining small hand specimens with the freshest possible vitric products for a petrological study. For heavy mineral separation, the leftovers of these hand specimens were later combined to provide sufficient material for a statistically meaningful number of analyses.

Sample 15BSK009 (Second Coast, Gruinard Bay; 57.86107° N, 5.49795° W) is a well-sorted, fine-grained sandstone of the Poll à Mhuilt Member lacustrine sequence immediately overlying the Stac Fada Member.

Sample 15BSK001 (Enard Bay; 58.07096° N, 5.35579° W) is a trough cross-bedded sandstone and is the stratigraphically highest

sample. It was collected from the Meall Dearg Formation, which represents a return to fluvial sedimentation above the Poll à Mhuilt Member of the Bay of Stoer Formation.

4.b. Analytical methods

Zircon and apatite grains were separated from whole-rock samples using crushing, milling, wet shaking table, heavy liquid and magnetic separation techniques at Trinity College Dublin. A selection of zircon grains from each sample were placed on conducting carbon tabs and their exteriors were imaged in backscatter electron (BSE) mode on a Tescan Mira XMU Field Emission Scanning Electron Microscope (SEM) at the Irish Centre for Research in Applied Geosciences (iCRAG) laboratory at Trinity College Dublin. A larger number of zircon and apatite grains were picked and were mounted in 2.5 cm diameter epoxy mounts. The mounts were polished with 6 and 1 µm diamond polishing paste to reveal the grain midsections. After application of a carbon coat of *c.* 10 nm thickness to the mounts, all zircon grains were imaged in cathodoluminescence (CL) mode using a KE Developments Centaurus system attached to the SEM. An accelerating voltage of 10 kV and working distance of *c.* 10 mm were used. Following removal of the carbon coat with a very brief (*c.* 30 s) polish using 1 µm diamond polishing paste, the zircon and apatite grains underwent laser ablation inductively coupled plasma mass spectrometry (LA-ICP-MS) U–Th–Pb analysis.

All zircon analyses were conducted on a Photon Machines Analyte Excite 193 nm ArF Excimer laser coupled to a Thermo Scientific iCAP-Qc ICP-MS at the Department of Geology, Trinity College Dublin, in a single analytical period (December 2015). The methodology closely followed that of Rodrigues *et al.* (2015). The laser produced a circular spot 30 µm in diameter and operated with a nominal fluence of 2.5 J cm⁻² for 180 shots at a 4 Hz laser repetition rate. Nine isotopes were measured during the analyses (⁸⁸Sr [3], ⁹¹Zr [3], ²⁰²Hg [2.5], ²⁰⁴Pb [50], ²⁰⁶Pb [50], ²⁰⁷Pb [70], ²⁰⁸Pb [50], ²³²Th [20] and ²³⁸U [40], where the numbers in square brackets represent the dwell time in milliseconds for each isotope; total cycle time of 288.5 ms). The 91500 standard zircon – ²⁰⁶Pb/²³⁸U isotope dilution thermal ionization mass spectrometry (ID-TIMS) age of 1062.4 ± 0.8 Ma (all uncertainties in the text are quoted at the 2σ level unless otherwise stated; Wiedenbeck *et al.* 1995) – was used as the calibration reference material (RM). Temora 2 – ²⁰⁶Pb/²³⁸U TIMS age of 416.78 ± 0.33 Ma (Black *et al.* 2004) – was analysed as a quality control material (QCM). Zircon QCM data for all sessions are shown in online Supplementary Appendix 1 (available at <http://journals.cambridge.org/geo>). The raw isotope data were reduced using the VizualAge data reduction scheme (DRS; Paton *et al.* 2010; Petrus & Kamber, 2012) in the IOLITE package (v. 2.5) of Paton *et al.* (2011). Processed data were plotted in the Isoplot 4.15 add-in (Ludwig, 2012) for Microsoft Excel.

Apatite U–Pb analyses were conducted over two separate analytical periods (December 2015 and September 2016). The analyses performed during the first analytical period (on samples 15BSK001 and 15BSK009) were conducted on the same LA-ICP-MS system as described above, following the procedure of Chew *et al.* (2014). A circular spot of 60 µm diameter was ablated for 225 shots at 5 Hz. The analyses performed during the second analytical period (on samples 15BSK006, 15BSK008 and 15BSK_X_SFM) were conducted on the same laser ablation system, which was on this occasion coupled to an Agilent 7900 ICP-MS. For these analyses, a circular spot 60 µm in diameter was used and the laser operated

with a fluence of 3.25 J cm^{-2} for 280 shots at a 10 Hz laser repetition rate. During the first analytical period, 34 isotopes were measured during the analyses (^{24}Mg [10], ^{31}P [5], ^{35}Cl [30], ^{43}Ca [25], ^{51}V [10], ^{55}Mn [10], ^{71}Ga [10], ^{73}Ge [10], ^{75}As [10], ^{88}Sr [20], ^{89}Y [5], ^{90}Zr [10], ^{139}La [5], ^{140}Ce [5], ^{141}Pr [5], ^{146}Nd [5], ^{147}Sm [10], ^{153}Eu [10], ^{157}Gd [10], ^{159}Tb [10], ^{163}Dy [10], ^{165}Ho [10], ^{166}Er [10], ^{169}Tm [10], ^{172}Yb [10], ^{175}Lu [10], ^{182}W [10], ^{202}Hg [10], ^{204}Pb [25], ^{206}Pb [60], ^{207}Pb [65], ^{208}Pb [10], ^{232}Th [20] and ^{238}U [40], where the numbers in square brackets represent the dwell time in milliseconds for each isotope; total dwell time of 515 ms). During the second analytical period, 29 isotopes were measured (as above, but excluding ^{24}Mg , ^{31}P , ^{71}Ga , ^{73}Ge and ^{182}W). Apatite rare earth element abundance data are provided alongside U–Pb data in online Supplementary Appendix 1. For all apatite analyses, a crystal of Madagascar apatite of size *c.* 1 cm (Thomson *et al.* 2012; an in-house aliquot of fragments of this crystal has yielded a weighted average ID-TIMS concordia age of 473.5 ± 0.7 Ma) was used as the RM, and McClure Mountain apatite ($^{207}\text{Pb}/^{235}\text{U}$ TIMS age of 523.51 ± 1.53 Ma; Schoene & Bowring, 2006) was analysed as a QCM. Apatite QCM data for all sessions are provided in online Supplementary Appendix 1. The raw isotope data were reduced using the VizualAge_UcomPbine DRS (Chew *et al.* 2014) in Iolite (Paton *et al.* 2011).

Unlike zircon, which excludes common (i.e. initial or non-radiogenic) Pb (Pb_c) during crystallization, apatite often has considerable Pb_c contents that can result in significant discordance in the U–Pb system. This is coupled with generally low U contents resulting in apparent lesser accumulation of radiogenic Pb (Pb^*), hence resulting in high Pb_c/Pb^* ratios that might hinder the dating of certain grains. Pb_c in the Madagascar apatite RM was corrected for using a ^{207}Pb -based method employing the known $^{207}\text{Pb}/^{206}\text{Pb}$ ratio (Chew *et al.* 2014). However, detrital apatite has by definition been isolated from co-genetic low-U phases that might have been used to estimate the initial Pb isotopic composition of the grain; the initial Pb isotopic composition must therefore be estimated from Pb evolution models. In this study, variable Pb_c in individual detrital apatite grains was corrected for by: (i) using a starting estimate for the age of the grain; (ii) calculating its corresponding initial Pb isotopic composition in the model of Stacey & Kramers (1975); and then (iii) adopting an iterative approach utilizing a ^{207}Pb correction, based on the procedure of Chew *et al.* (2011).

5. Results

5.a. Shock features in zircon

External and internal imaging of zircon grains from all samples showed little evidence of potential shock features. A single grain in sample 15BSK001, stratigraphically above the Stac Fada Member, displayed planar microstructures that may be impact-related (Fig. 3a–c). In zircon, no neoblasts or granular textures, potentially related to impact-induced recrystallization, were observed. Such features have been shown to record the impact age at a number of impact structures (e.g. Vredefort, South Africa, Moser, 1997; Moser *et al.* 2011; Cavosie *et al.* 2015; Sudbury, Canada, Kenny *et al.* 2017; Nicholson Lake, Canada, McGregor *et al.* 2018; Lappajärvi, Finland, Kenny *et al.* 2019) and would provide an opportunity to obtain the first direct U–Pb age for the impact event related to the Stac Fada Member deposits if they could be identified. The apparent rarity of shock

features in zircon in the samples studied here is consistent with the observation of Osinski *et al.* (2011) that some samples of the Stac Fada Member contain no shocked quartz and, in general, the unit appears to contain an order of magnitude less shocked material than proximal impact melt-bearing ejecta layers (such as suevite from the Ries impact structure, Germany; e.g. Engelhardt, 1997).

5.b. Zircon U–Pb age data

All zircon and apatite U–Pb data from this study can be found in online Supplementary Appendix 1. Studies of detrital zircon generally exclude analyses with discordance greater than an arbitrary cut-off value from consideration (e.g. Fedo *et al.* 2003); here, analyses that were > 10% discordant (grey ellipses in Fig. 4) were not considered further.

The five analysed samples of the Stoer Group display very similar zircon age distributions (Figs 4–6). Their age populations are all dominated by a major peak at 2.9–2.7 Ga with minor populations at *c.* 3.2–3.1 Ga, *c.* 2.5 Ga, *c.* 2.4 Ga, *c.* 1.9 Ga and *c.* 1.75 Ga (Figs 4, 5). The youngest concordant analyses are from two grains in sample 15BSK009, which have $^{206}\text{Pb}/^{238}\text{U}$ ages of 1.43 ± 0.02 Ga and 1.23 ± 0.02 Ga, and a grain in sample 15BSK_X_SFM, which has a $^{206}\text{Pb}/^{238}\text{U}$ age of 1.24 ± 0.01 Ga. Overall, the detrital zircon U–Pb distributions for the Stoer Group reported here are very similar to those reported by Rainbird *et al.* (2001) and Kinnaird *et al.* (2007); however, the higher number of analyses here (a total of 553 analyses that were < 10% discordant, compared with 127 and 16, respectively, in the previous studies) has allowed additional insights. For example, the youngest detrital zircon ages encountered here are significantly younger than the > 1.7 Ga ages reported previously. However, we note that caution should be applied when interpreting single detrital zircon analyses, particularly in the interpretation of youngest ages as, for example, post-sedimentation Pb loss may result in erroneously young ages (Nelson, 2001). Additionally, this study confirms the presence of a distinct *c.* 3.2–3.1 Ga population (which was previously represented by only a single < 10% discordant analysis) and reports the first Palaeoarchaeon age for a zircon grain from the Stoer Group; the oldest concordant analysis in this study has a $^{207}\text{Pb}/^{206}\text{Pb}$ age of 3529 ± 30 Ma (Fig. 4d inset; online Supplementary Appendix 1). With a total of 696 < 10% discordant zircon U–Pb analyses for the Stoer Group from this and previous studies (Rainbird *et al.* 2001; Kinnaird *et al.* 2007; Fig. 7), there is now 95% confidence that no fractions of the zircon population composing $\geq 1.2\%$ of the total have been missed (cf. Vermeesch, 2004).

Visual comparison of the samples on histograms and kernel density estimates (Fig. 5), as well as cumulative distribution function (CDF) and quantile-quantile (QQ) plots (Fig. 6), show that 15BSK006 (the stratigraphically lowest and geographically most northern sample) is the single sample with a noticeable, although still only slight, difference in zircon age distribution. This observation is supported by the results of a Kolmogorov–Smirnov (K-S) statistical test which demonstrates that only sample 15BSK006 is statistically likely (at a 95% confidence level) to have been sourced from a different population than any of the other samples (online Supplementary Appendix 2, Table S1A, available at <http://journals.cambridge.org/geo>). We note that in this study the K-S test results support observations that were first made by visual inspection but that, in general, the *P* value of the K-S test may be considered a poor

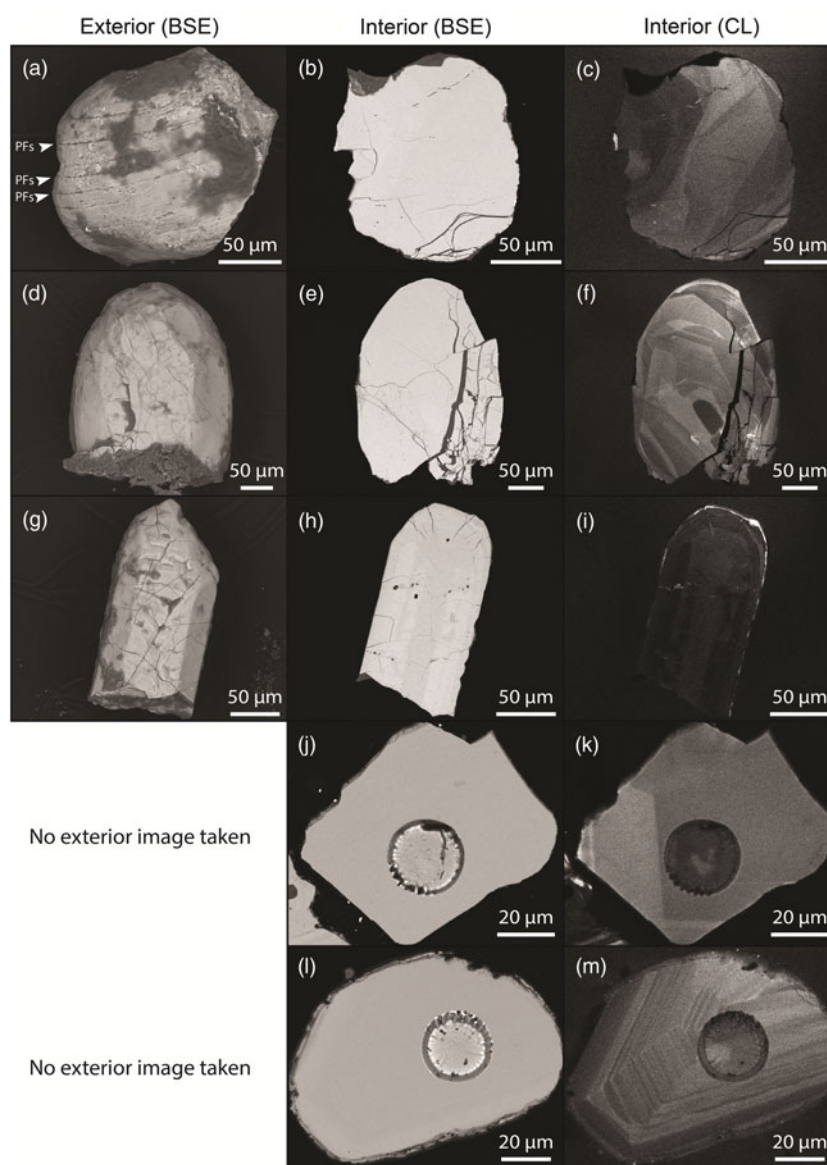


Fig. 3. (Colour online) Zircon imaging. (a–c) Zircon grain from sample 15BSK001 (taken from stratigraphically above the Stac Fada Member) which shows potentially impact-related planar microstructures on its exterior. (d–i) Two zircon grains that did not display any potentially impact-related textures (typical of most grains in this study). Both are from the Stac Fada Member itself. (j–m) The two youngest detrital zircon grains in the Stoer Group: grain 15BSK009/Z/41 (j, k) and grain 15BSK_X_SFM/Z/82 (l, m). Circular features are laser ablation U–Pb analysis pits. BSE – backscattered electron; CL – cathodoluminescence; PFs – planar fractures.

measure of dissimilarity between samples due to the strong dependence of results on sample size (Vermeesch, 2013). The reason that sample 15BSK006 appears to be distinct is largely as a result of it lacking the *c.* 1.9 Ga age population observed in all other samples.

5.c. Apatite U–Pb age data

Due to the nature of the ^{207}Pb -based correction for common Pb, no apatite U–Pb age data can be excluded on the basis of discordance. Instead, grains with ^{207}Pb -corrected 2σ age uncertainties above a certain threshold value (which may be absolute and/or a percentage) are not considered further (e.g. Zattin *et al.* 2012; Mark *et al.* 2016; O’Sullivan *et al.* 2016). Here, this value was set at 5%. This corresponds to an absolute age threshold similar to that employed in studies of mostly Phanerozoic-aged apatite grains, which are typically screened at 20% (e.g. O’Sullivan *et al.* 2018).

Similar to the zircon data, the five samples display comparable apatite age distributions (Figs 4–6). Visual inspection of the data on histograms and kernel density plots (Fig. 5), as well as CDF and QQ plots (Fig. 6), is again supported by K–S test results indicating no statistically significant difference in age distributions between samples (online Supplementary Appendix 2, Table S2). However, the age peaks are different to those in the zircon record; all samples display a range of ages between *c.* 2.6 and *c.* 2.15 Ga and a broad and dominant peak between *c.* 1.8 and *c.* 1.55 Ga, and most samples also have minor peaks centred at *c.* 1.4 and *c.* 1.15 Ga (Fig. 5). Sample 15BSK006, which appeared to be the most distinctive in terms of zircon U–Pb age distribution, is the only sample that lacks apatite grains younger than 1500 Ma.

Two apatite grains in the filtered dataset (339 grains in five samples) have ^{207}Pb -corrected U–Pb ages (1101 ± 38 Ma and 1109 ± 40 Ma) that are younger than the current estimate for the deposition of the Stac Fada Member: a 1177 ± 5 Ma $^{40}\text{Ar}/^{39}\text{Ar}$ age for

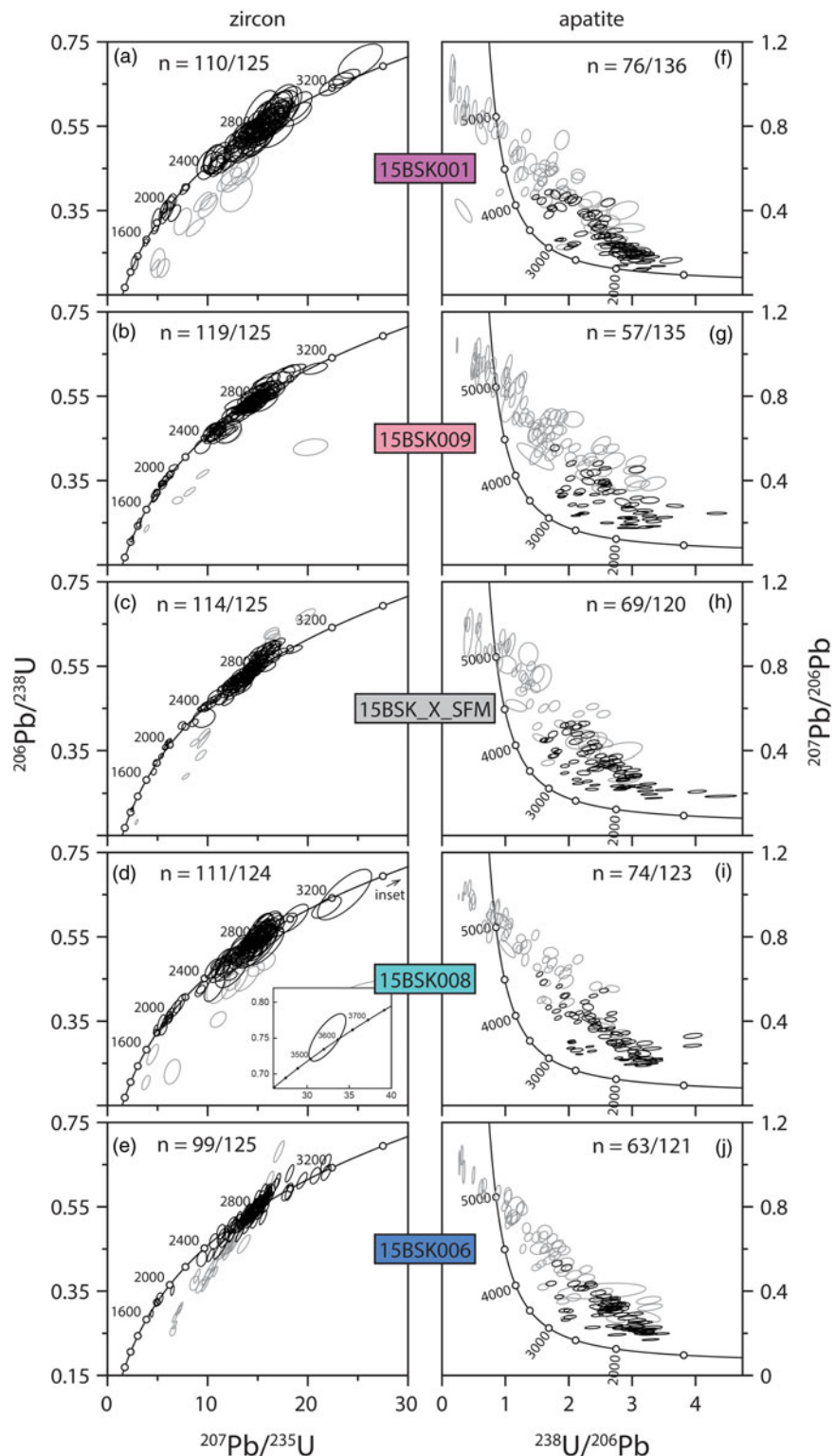


Fig. 4. (Colour online) Concordia diagrams for detrital zircon (left panels) and apatite U-Pb data (right panels). For zircon data, grey ellipses represent analyses that are more than 10% discordant. For apatite data, grey ellipses represent analyses for which the 2σ uncertainty on the ^{207}Pb -corrected age was greater than 5%. Number of concordant (for zircon) or low uncertainty (for apatite) analyses v. total number of grains analysed given for each sample.

authigenic K-feldspar which precipitated in degassing structures in the Stac Fada Member itself (Parnell *et al.* 2011). Both of these grains are from sample 15BSK008, which was taken from stratigraphically below the Stac Fada Member (Fig. 2). The two grains

which gave ages younger than the currently accepted age of deposition for the unit may be explained by, for example, (i) subtle Pb loss from these two crystals; or (ii) inaccuracy in the $^{40}\text{Ar}/^{39}\text{Ar}$ age. The latter appears unlikely given the robust nature of the

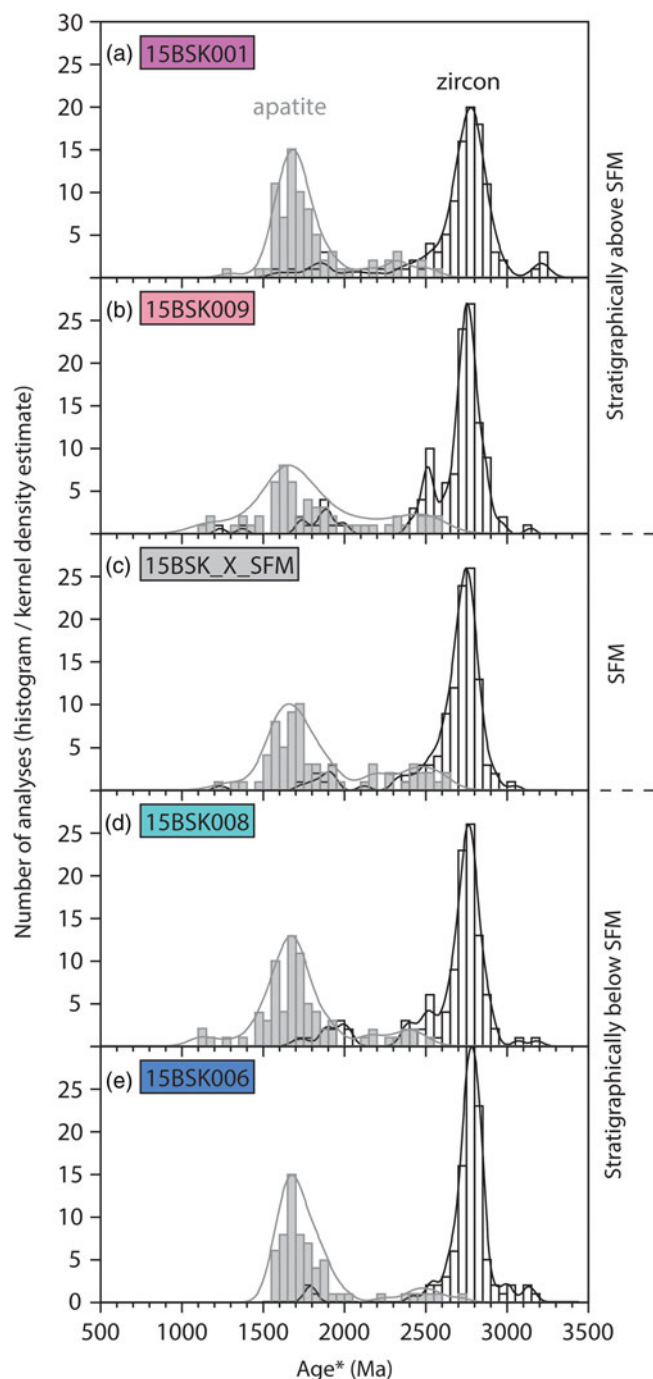


Fig. 5. (Colour online) Detrital zircon and apatite U–Pb age distributions. Zircon data are $^{207}\text{Pb}/^{206}\text{Pb}$ ages for analyses which were less than 10% discordant, whereas apatite data are ^{207}Pb -corrected apatite U–Pb ages which had 2σ age uncertainties less than 5% (black ellipses in Fig. 4). Kernel density estimates were plotted using the DensityPlotter program of Vermeesch (2012), in which the optimal bandwidth is calculated according to the method of Botev *et al.* (2010). SFM – Stac Fada Member.

$^{40}\text{Ar}/^{39}\text{Ar}$ results from samples from a number of localities. Regardless, the presence of shock metamorphosed zircon in the unit (Reddy *et al.* 2015) suggests that there may also be the possibility for future studies to obtain a direct U–Pb age for the impact event through analysis of shocked accessory phases such as zircon (e.g. Bohor *et al.* 1993; Krogh *et al.* 1993a,b; Kamo *et al.* 1996; Moser, 1997; Moser *et al.* 2011; Cavosie *et al.* 2015; Kenny *et al.*

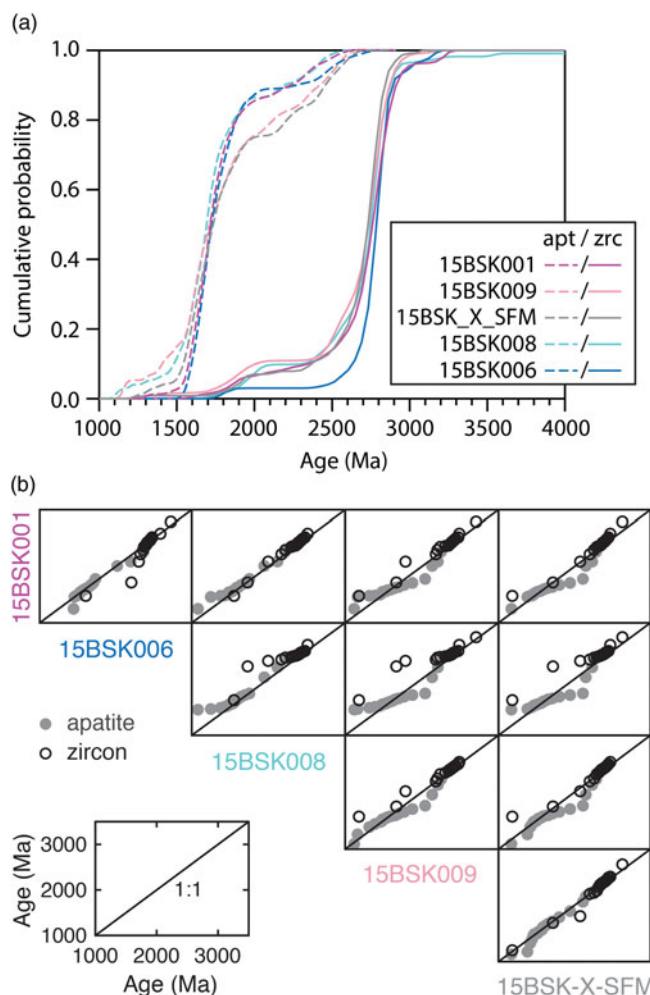


Fig. 6. (Colour online) Cumulative distribution function (CDF) and quantile-quantile (QQ) plots for detrital zircon $^{207}\text{Pb}/^{206}\text{Pb}$ ages and detrital apatite ^{207}Pb -corrected ages. (a) apt – apatite; zrc – zircon. (b) Dots represent the 0, 5, 10, . . . , 95 and 100 percentiles (or quantiles) of the samples whose names are shown on the x- and y-axis, respectively. A pair of samples have identical distributions if their percentiles fall on the 1:1 line (Vermeesch, 2013).

2017, 2019; McGregor *et al.* 2018), monazite (e.g. Erickson *et al.* 2017) or baddeleyite (e.g. White *et al.* 2017).

6. Discussion

6.a. Stratigraphic variation

The lack of significant stratigraphic variations in zircon or apatite U–Pb age distributions through the Stoer Group, NW Scotland, may be interpreted as evidence that there was no major change in the source of detritus during Stoer Group deposition. Alternatively, there may have been a significant change in sediment source, but it could not be detected as the different source regions shared similar apatite and zircon U–Pb age populations.

The polycyclic nature of zircon and the ability of intermediate repositories to overwhelm local provenance (e.g. Sircombe & Freeman, 1999) mean that changes in sedimentary provenance throughout a succession may not necessarily result in any major change in the detrital zircon age distribution. Apatite, by contrast, is more likely to represent first-cycle detritus (Morton &

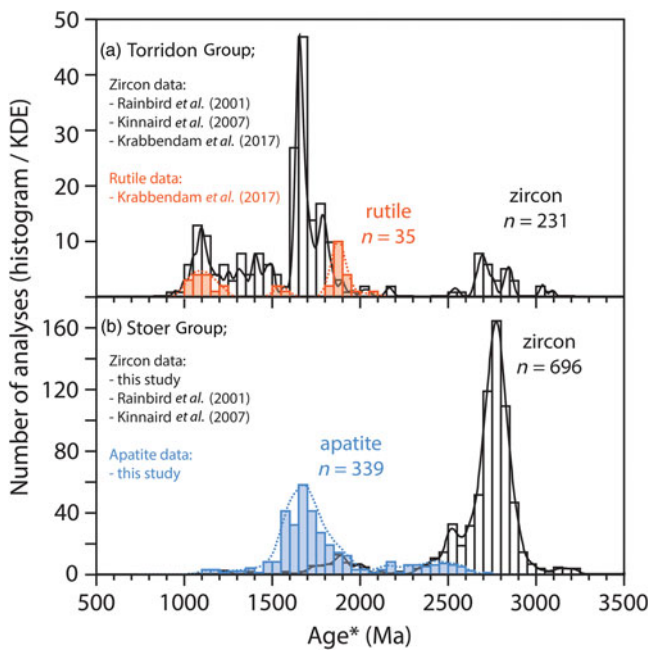


Fig. 7. (Colour online) Compiled detrital zircon, apatite and rutile U–Pb age distributions for the Stoer and Torridon groups. Note that zircon and rutile data for the Torridon Group from Krabbendam *et al.* (2017) are only from sample ZY320 (which was taken at Gruinard Bay, near sample GY96-56 of Rainbird *et al.* 2001; Krabbendam *et al.* 2017, p. 76), and therefore do not include data for sample ZY327 of Krabbendam *et al.* (2017), which was taken approximately 60 km further south. Zircon and rutile data are $^{207}\text{Pb}/^{206}\text{Pb}$ ages for analyses that were less than 10% discordant, whereas apatite data are ^{207}Pb -corrected apatite U–Pb ages that had 2σ age uncertainties less than 5%. KDE – kernel density estimate.

Hallsworth, 1999) and may therefore be more likely than zircon to record major shifts in provenance throughout a succession. The relatively constant nature of detrital apatite U–Pb age distributions across the Stac Fada Member may therefore lend support to the first explanation, that is, there was no major shift in drainage pattern.

Consistency in detrital zircon and apatite U–Pb age distributions throughout a stratigraphic section could conceivably be related to extensive reworking of underlying sediments. The lower part of the Stoer Group appears to have been deposited in a series of narrow, high-gradient bedrock and alluvial valleys that were only partially connected, whereas the younger parts of the Stoer Group appear to have been deposited in broader, low-gradient alluvial settings, with aeolian processes on-going in areas far from basement highs (Ielpi *et al.* 2016). It has been suggested that this transition in the Stoer Group led to more mature and hydrologically open drainage that was capable of remobilizing fine-grained detritus, with “mobilization and reworking of sandy detritus in extra-channel areas also enhanced by the absence of plant rooting” (Went, 2005; Ielpi *et al.* 2016, p. 309).

The zircon and apatite U–Pb age results need to be considered in the context of palaeocurrent data for the Stoer Group. The well-documented changes in flow direction throughout the unit – from variable palaeocurrent directions below the Stac Fada Member, to broadly eastwards movement in the up to 100 m thick lacustrine sedimentary rocks of the Poll à Mhuilt Member immediately overlying the Stac Fada Member, to broadly westwards flow directions in the post-Poll à Mhuilt Member (Stewart, 2002; Simms, 2015) – indicate that there was at least some change in the regional drainage network coincident with the deposition of the Stac Fada Member.

Regardless of whether the relatively constant age distributions of heavy minerals in the Stoer Group can be interpreted as indicative of a lack of major shift in sediment source, they do not provide independent evidence that the impact associated with the Stac Fada Member: (i) brought previously unexposed rocks to the Earth’s surface; (ii) cut off specific source terrain(s); or (iii) resulted in any major change in the regional Stoer Group sedimentary system that might indicate a location of the impact structure.

The very minor differences between the U–Pb age spectra may be related to geographic or stratigraphic factors. For example, the lack of *c.* 1.9 Ga zircon grains in sample 15BSK006 may be related to this sample’s northernmost location (Fig. 1) or its lowermost stratigraphic position of the five studied samples (Fig. 2). Interestingly, Rainbird *et al.* (2001) identified two *c.* 1.9 Ga zircon grains ($^{207}\text{Pb}/^{206}\text{Pb}$ ages of 1866 ± 62 and 1912 ± 30 Ma) in samples from even lower in the Stoer Group stratigraphy at the relatively southern location of Gruinard Bay. This may indicate that the absence of *c.* 1.9 Ga zircon grains in sample 15BSK006 is not related to stratigraphic position and may, more conceivably, be related to the sample’s geographic location. Additionally, intrusions of *c.* 1.9 Ga age are mainly found close to Lewisian terrane boundaries, for example, the Ard gneiss in the Gairloch area to the south (Park *et al.* 2001) and the Ben Stack granites near Loch Laxford to the north (Goodenough *et al.* 2013). Sample 15BSK006 is the sample most distal to these known *c.* 1.9 Ga intrusions, and we suggest that this is the most likely reason for its lack of grains of this age.

6.b. Provenance

6.b.1. Detrital zircon

The new zircon U–Pb data for the Stoer Group are consistent with the U–Pb data of Rainbird *et al.* (2001) and Kinnaird *et al.* (2007) and earlier interpretations that the detritus was largely derived from local Lewisian Gneiss Complex basement (e.g. Stewart, 1982, 1990, 2002; Van de Kamp & Leake, 1997). Rainbird *et al.* (2001) noted that the major detrital zircon age peak at 2.9–2.7 Ga corresponds to protolith ages for rocks of the Lewisian Gneiss Complex in the Gruinard Bay area (Whitehouse *et al.* 1997; Corfu *et al.* 1998) as well as high-grade metamorphic events in the north–central part of the Lewisian. However, recent work has shown that complex polyphase metamorphism of the Lewisian has resulted in zircon U–Pb ages distributed along the concordia between *c.* 3.0 Ga and *c.* 2.5 Ga; it is therefore difficult to ascribe specific protolith ages within this time (Whitehouse & Kemp, 2010; MacDonald *et al.* 2015). We observe this broad spread of data in the Stoer Group (Figs 4, 5). The zircon peak at *c.* 2.5 Ga (Fig. 7b) corresponds to the 2490–2480 Ma Inverian event of the Lewisian central region (Humphries & Cliff, 1982; Corfu *et al.* 1994) and the peak at *c.* 1.9 Ga corresponds to felsic magmatism and metamorphism at a number of localities in the Lewisian at approximately this time, including the South Harris Complex, the Ben Stack granites and the Ard gneiss (e.g. Park *et al.* 2001; Whitehouse & Bridgwater, 2001; Mason *et al.* 2004; Goodenough *et al.* 2013). Rare zircon grains with ages of *c.* 1.7 Ga are likely related to pegmatites that intruded into most of the Lewisian at this time (e.g. Park *et al.* 2001). It is also possible that there was a small contribution of material from distal sources to the west, which became more prevalent by the time of deposition of the Sleat and Torridon groups (Fig. 7a; Krabbendam *et al.* 2017).

The detrital populations in the Stoer Group not previously identified (including grains at *c.* 3.5 Ga and *c.* 3.2–3.1 Ga, as well as Mesoproterozoic ages) can also be attributed to sources in the Lewisian Gneiss Complex. The Palaeoarchaeic ages reported from the Stoer Group (3529 ± 30 Ma) may be related to the *c.* 3550 Ma inherited core found in a grain from the northern part of the Lewisian Gneiss Complex (Kinny & Friend, 1997). Similarly, the few *c.* 3.2–3.1 Ga analyses may be related to the 3115 ± 18 Ma analysis on a zircon core from the central region of the Lewisian Gneiss Complex (Kinny & Friend, 1997).

6.b.2. Detrital apatite

The U–Pb age distribution of detrital apatite in the Stoer Group contrasts starkly with that of zircon (Fig. 7). Some of the apatite ages are likely to be related to rocks and events known from the zircon record (with the former potentially offset to younger ages due to the lower closure temperature of its U–Pb system), but others are likely related to previously unrepresented events.

The main apatite age peak, centred at *c.* 1.7 Ga, represents cooling from amphibolite-facies metamorphism of the Laxfordian event, which is recorded in the Lewisian Gneiss Complex by titanite and rutile ages (Heaman & Tarney, 1989; Corfu *et al.* 1994; Kinny & Friend, 1997; Love *et al.* 2010), as well as rare zircon rims (Kinny & Friend, 1997). This event is not well-represented in zircon in the Stoer Group (Fig. 7), consistent with it being a low-temperature metamorphic event but, as noted above, the few *c.* 1.7 Ga zircon grains we observed may have been sourced from pegmatites associated with Laxfordian metamorphism (Park *et al.* 2001).

Considering the broad distribution of apatite ages between 2.6 and 2.1 Ga, it is noteworthy that zircon, by contrast, is relatively scarce between 2.4 and 2.1 Ga but represented by a clear peak at *c.* 2.5 Ga (Fig. 7b). Some of the younger apatite ages may be related to discrete events not recorded by zircon (e.g. at *c.* 2.15 Ga), but others most likely represent prolonged cooling and exhumation after the 2490–2480 Ma high-grade Inverian metamorphism in the central region of the Lewisian Gneiss Complex.

Finally, the almost complete absence of > 2.5 Ga apatite ages in the Stoer Group, despite the abundance of zircon of this age, is most easily explained by the resetting of the U–Pb system in apatite by relatively low-grade metamorphic events having affected the source rocks. Rocks with Archaean zircon U–Pb ages may yield Proterozoic apatite U–Pb ages if they are heated to temperatures above the partial retention window for Pb in apatite (*c.* 375–450°C), but not sufficiently high to reset the zircon U–Pb systematics.

6.b.3. Youngest detrital grains

Considering the youngest detrital mineral ages measured in the Stoer Group, the two zircon grains which gave *c.* 1.25 Ga ages (and are within 2σ analytical uncertainty of the 1177 ± 5 Ma $^{40}\text{Ar}/^{39}\text{Ar}$ age for authigenic K-feldspar in the Stac Fada Member; Parnell *et al.* 2011) are likely to represent the same source as the small number of apatite grains with *c.* 1.2 Ga ages (Fig. 7b). The two youngest zircon grains lack any evidence for shock features typical of impact-induced age resetting (Fig. 3j–m), such as granular textures (e.g. Bohor *et al.* 1993; Krogh *et al.* 1993a,b; Kamo *et al.* 1996; Moser, 1997; Moser *et al.* 2011; Cavosie *et al.* 2015; Kenny *et al.* 2017, 2019; McGregor *et al.* 2018). Together with the lack of evidence for impact-related U–Pb discordance in the dataset in general (Fig. 4), this suggests that these youngest ages are not related to Pb loss or recrystallization associated with the Stac Fada Member impact event itself. In addition to inducing

shock deformation and age resetting in zircon, medium to large impact events can also crystallize new igneous zircon and apatite in slowly cooled impact melts (e.g. at Vredefort, South Africa, Kamo *et al.* 1996; Sudbury, Canada, Davis, 2008; Manicouagan, Canada, Hodych & Dunning, 1992; Morokweng, South Africa, Hart *et al.* 1997; Koeberl *et al.* 1997; and Mistastin Lake, Canada, Sylvester *et al.* 2013). However, to the best of our knowledge, zircon which crystallized from impact melt has not previously been reported in distal impact deposits and, given the time required for zircon to first crystallize from an impact melt, such an occurrence seems unlikely. Although it cannot be ruled out entirely, an impact melt origin appears similarly unlikely for the single *c.* 1.25 Ga zircon grain in the overlying Poll à Mhuil Member (Fig. 5d).

We note that the Stoer Group is generally considered to have been deposited prior to the Grenville Orogeny in Scotland (Stewart, 2002), which is dated to *c.* 1.1–1.0 Ga (e.g. Sanders *et al.* 1984; Brewer *et al.* 2003), and the youngest detrital grains are therefore unlikely to be related to even very early Grenvillian orogenesis. However, ages of between 1.1 and 1.3 Ga have previously been reported from the Lewisian Gneiss Complex – early Rb–Sr and K–Ar biotite ages fall in the range of *c.* 1148–1169 Ma (Giletti *et al.* 1961; Moorbath & Park, 1972) – and there are a number of more distal possible sources for the *c.* 1.25 Ga grains (e.g. the Gardar Province of South Greenland; Upton *et al.* 2003). In conclusion, there is no single clear source for the youngest detrital grains in the Stoer Group.

7. Conclusions

Minimal evidence for shock metamorphism or associated Pb loss in zircon or apatite was encountered in this study. Despite extensive efforts at SEM imaging, potentially impact-related planar fractures were only identified on the exterior of a single zircon grain. Although a number of zircon and apatite grains in the Stoer Group yielded U–Pb ages within uncertainty of the 1177 ± 5 Ma $^{40}\text{Ar}/^{39}\text{Ar}$ depositional age constraint for the Stac Fada Member, neither of the two such zircon grains displayed textures indicative of shock metamorphism and, overall, there was no clear evidence for impact-induced Pb loss in the dataset.

The new zircon U–Pb data for the Stoer Group reported here are consistent with earlier interpretations that the detritus was derived largely from local Lewisian Gneiss Complex basement, but the larger number of analyses in this study resulted in the identification of ages previously undocumented in the Stoer Group; these include grains at *c.* 3.5 Ga (the first Palaeoarchaeic ages reported from the Stoer Group) and *c.* 3.2–3.1 Ga, as well as Mesoproterozoic ages.

Detrital zircon and apatite in the Stoer Group display contrasting age distributions. The first apatite age data for the Stoer Group highlights events either underrepresented in or absent from the zircon record, with the apatite record dominated by the *c.* 1.7 Ga Laxfordian event. Conversely, detrital apatite U–Pb fails to record events older than *c.* 2.5 Ga, indicating that all rocks in the sediment source regions older than 2.5 Ga have been heated above the closure temperature of the apatite U–Pb system (*c.* 375–450°C).

Neither zircon nor apatite recorded significant changes in U–Pb age distribution across the impact-related Stac Fada Member of the Stoer Group, NW Scotland. The U–Pb systems in detrital apatite and zircon assemblages do not provide independent support for a major shift in regional drainage patterns associated with the Stac

Fada Member impact event, and as such, do not yield any information on the likely location of the impact structure.

Supplementary material. To view supplementary material for this article, please visit <https://doi.org/10.1017/S0016756819000220>.

Author ORCIDs.  Gavin Kenny, 0000-0001-8683-3860

Acknowledgements. This research was supported by an Irish Research Council EMBARK Initiative scholarship (GGK) and funding from Science Foundation Ireland (SFI) (BSK, grant no. SFI/12/ERC/E2499). The U–Pb data in this publication were obtained on infrastructure supported in part by a research grant from SFI (grant no. 13/RC/2092) and co-funded under the European Regional Development Fund and industry partners of the Irish Centre for Research in Applied Geosciences (iCRAG). The SEM data in this publication were obtained on infrastructure supported in part by a research grant from SFI (BSK, grant no. SFI/RI/3227). We thank reviewers Kathryn Goodenough and Maarten Krabbendam for their constructive feedback and Chad Deering for efficient editorial handling.

Declaration of interest. None.

References

- Amor K, Hesselbo SP, Porcelli D, Thackrey S and Parnell J (2008) A Precambrian proximal ejecta blanket from Scotland. *Geology* **36**, 303–6.
- Amor K, Taylor J, Hesselbo SP and MacNiocaill C (2011) An anisotropy of magnetic susceptibility study of the Stac Fada Member suevite: constraints on the impact crater location. *Meteoritics & Planetary Science* **46**, A10.
- Binns PE, McQuillan R, Fannin NGT, Kenolty N and Ardu DA (1975) Structure and stratigraphy of sedimentary basins in the Sea of the Hebrides and the Minches. In *Petroleum and the Continental Shelf of North-West Europe* (ed. AW Woodland), pp. 93–102. Barking: Applied Science Publishers.
- Black LP, Kamo SL, Allen CM, Davis DW, Aleinikoff JN, Valley JW, Mundil R, Campbell IH, Korsch RJ, Williams IS and Foudoulis C (2004) Improved ²⁰⁶Pb/²³⁸U microprobe geochronology by the monitoring of a trace-element-related matrix effect; SHRIMP, ID–TIMS, ELA–ICP–MS and oxygen isotope documentation for a series of zircon standards. *Chemical Geology* **205**, 115–40.
- Bohor B, Betterton W and Krogh T (1993) Impact-shocked zircons: discovery of shock-induced textures reflecting increasing degrees of shock metamorphism. *Earth and Planetary Science Letters* **119**, 419–24.
- Botev ZI, Grotowski JF and Kroese DP (2010) Kernel density estimation via diffusion. *The Annals of Statistics* **38**, 2916–57.
- Bouch JE, Hole MJ, Trewin NH, Chenery SP and Morton AC (2002) Authigenic apatite in a fluvial sandstone sequence: evidence for rare-earth element mobility during diagenesis and a tool for diagenetic correlation. *Journal of Sedimentary Research* **72**, 59–67.
- Branney MJ and Brown RJ (2011) Impactoclastic density current emplacement of terrestrial meteorite-impact ejecta and the formation of dust pellets and accretionary lapilli: evidence from Stac Fada, Scotland. *The Journal of Geology* **119**, 275–92.
- Brewer TS, Storey CD, Parrish RR, Temperley S and Windley BF (2003) Grenvillian age decompression of eclogites in the Glenelg–Attadale Inlier, NW Scotland. *Journal of the Geological Society* **160**, 565–74.
- British Geological Survey (2002) *Point of Stoer, Scotland Sheet 107W*. Keyworth, Nottingham: Solid and Drift Geology.
- Cavosie AJ, Erickson TM, Timms NE, Reddy SM, Talavera C, Montalvo SD, Pincus MR, Gibbon RJ and Moser D (2015) A terrestrial perspective on using ex situ shocked zircons to date lunar impacts. *Geology* **43**, 999–1002.
- Chew DM, Petrus JA and Kamber BS (2014) U–Pb LA–ICPMS dating using accessory mineral standards with variable common Pb. *Chemical Geology* **363**, 185–99.
- Chew DM, Sylvester PJ and Tubrett MN (2011) U–Pb and Th–Pb dating of apatite by LA–ICPMS. *Chemical Geology* **280**, 200–16.
- Corfu F, Crane A, Moser D and Rogers G (1998) U–Pb zircon systematics at Gruinard Bay, northwest Scotland: implications for the early orogenic evolution of the Lewisian complex. *Contributions to Mineralogy and Petrology* **133**, 329–45.
- Corfu F, Heaman LM and Rogers G (1994) Polymetamorphic evolution of the Lewisian Complex, NW Scotland, as recorded by U–Pb isotopic compositions of zircon, titanite and rutile. *Contributions to Mineralogy and Petrology* **117**, 215–28.
- Davis DW (2008) Sub-million-year age resolution of Precambrian igneous events by thermal extraction–thermal ionization mass spectrometer Pb dating of zircon: Application to crystallization of the Sudbury impact melt sheet. *Geology* **36**, 383–6.
- Drake SM, Beard AD, Jones AP, Brown DJ, Fortes AD, Millar IL, Carter A, Baca J and Downes H (2017) Discovery of a meteoritic ejecta layer containing unmelted impactor fragments at the base of Paleocene lavas, Isle of Skye, Scotland. *Geology* **46**, 171–4.
- Engelhardt W (1997) Suevite breccia of the Ries impact crater, Germany: Petrography, chemistry and shock metamorphism of crystalline rock clasts. *Meteoritics & Planetary Science* **32**, 545–54.
- Erickson TM, Timms NE, Kirkland CL, Tohver E, Cavosie AJ, Pearce MA and Reddy SM (2017) Shocked monazite chronometry: integrating microstructural and in situ isotopic age data for determining precise impact ages. *Contributions to Mineralogy and Petrology* **172**, 11.
- Fedo CM, Sircombe KN and Rainbird RH (2003) Detrital zircon analysis of the sedimentary record. *Reviews in Mineralogy and Geochemistry* **53**, 277–303.
- Giletti BJ, Moorbath S and Lambert R (1961) A geochronological study of the metamorphic complexes of the Scottish Highlands. *Quarterly Journal of the Geological Society* **117**, 233–64.
- Goodenough KM, Crowley QG, Krabbendam M and Parry SF (2013) New U–Pb age constraints for the Laxford Shear Zone, NW Scotland: Evidence for tectono-magmatic processes associated with the formation of a Paleoproterozoic supercontinent. *Precambrian Research* **233**, 1–19.
- Goodenough KM and Krabbendam M (2011) *A geological excursion guide to the North-west Highlands of Scotland*. Edinburgh: Edinburgh Geological Society and NMS Enterprises.
- Grieve RA and Pilkington M (1996) The signature of terrestrial impacts. *AGSO Journal of Australian Geology and Geophysics* **16**, 399–420.
- Hart RJ, Andreoli MAG, Tredoux M, Moser D, Ashwal LD, Eide EA, Webb SJ and Brandt D (1997) Late Jurassic age for the Morokweng impact structure, southern Africa. *Earth and Planetary Science Letters* **147**, 25–35.
- Heaman LM and Tarney J (1989) U–Pb baddeleyite ages for the Scourie dyke swarm, Scotland: evidence for two distinct intrusion events. *Nature* **340**, 705.
- Hildebrand AR, Pilkington M, Ortiz-Aleman C, Chavez RE, Urrutia-Fucugauchi J, Connors M, Graniel-Castro E, Camara-Zi A, Halpenny JF and Niehaus D (1998) Mapping Chicxulub crater structure with gravity and seismic reflection data. In *Meteorites: Flux with Time and Impact Effects* (eds MM Grady, R Hutchison, GJH McCall and DA Rothery), pp. 59–73. Geological Society of London, Special Publication no. 140.
- Hodych JP and Dunning GR (1992) Did the Manicouagan impact trigger end-of-Triassic mass extinction? *Geology* **20**, 51–4.
- Humphries FJ and Cliff RA (1982) Sm–Nd dating and cooling history of Scourian granulites, Sutherland. *Nature* **295**, 515.
- Ielpi A, Ventra D and Ghinassi M (2016) Deeply channelled Precambrian rivers: Remote sensing and outcrop evidence from the 1.2 Ga Stoer Group of NW Scotland. *Precambrian Research* **281**, 291–311.
- Irving E and Runcorn K (1957) II. Analysis of the paleomagnetism of the Torridonian sandstone series of North-West Scotland. *Philosophical Transactions of the Royal Society of London: Series A, Mathematical and Physical Sciences* **250**, 83–99.
- Joosu L, Leland A, Kreitsmann T, Üpraus K, Roberts NMW, Paiste P, Martin AP and Kirsimäe K (2016) Petrography and the REE-composition of apatite in the Paleoproterozoic Pilgijärvi Sedimentary Formation, Pechenga Greenstone Belt, Russia. *Geochimica et Cosmochimica Acta* **186**, 135–53.
- Kamo SL, Reimold WU, Krogh TE and Colliston WP (1996) A 2.023 Ga age for the Vredefort impact event and a first report of shock metamorphosed zircons in pseudotachylitic breccias and Granophyre. *Earth and Planetary Science Letters* **144**, 369–87.

- Kenny GG, Morales LF, Whitehouse MJ, Petrus JA and Kamber BS (2017) The formation of large neoblasts in shocked zircon and their utility in dating impacts. *Geology* **45**, 1003–6.
- Kenny GG, Schmieder M, Whitehouse MJ, Nemchin AA, Morales LFG, Buchner E, Bellucci JJ and Snape JF (2019) A new U–Pb age for shock-recrystallised zircon from the Lappajärvi impact crater, Finland, and implications for the accurate dating of impact events. *Geochimica et Cosmochimica Acta* **245**, 479–94.
- Kinnaid TC, Prave AR, Kirkland CL, Horstwood M, Parrish R and Batchelor RA (2007) The late Mesoproterozoic–early Neoproterozoic tectonostratigraphic evolution of NW Scotland: the Torridonian revisited. *Journal of the Geological Society* **164**, 541–51.
- Kinny PD and Friend CRL (1997) U–Pb isotopic evidence for the accretion of different crustal blocks to form the Lewisian Complex of northwest Scotland. *Contributions to Mineralogy and Petrology* **129**, 326–40.
- Kirkham A (2003) Glauconitic spherules from the Triassic of the Bristol area, SW England: probable microtektite pseudomorphs. *Proceedings of the Geologists' Association* **114**, 11–21.
- Koerberl C, Armstrong RA and Reimold WU (1997) Morokweng, South Africa: A large impact structure of Jurassic–Cretaceous boundary age. *Geology* **25**, 731–4.
- Krabbendam M, Bonsor H, Horstwood MSA and Rivers T (2017) Tracking the evolution of the Grenvillian foreland basin: Constraints from sedimentology and detrital zircon and rutile in the Sleat and Torridon groups, Scotland. *Precambrian Research* **295**, 67–89.
- Krogh TE, Kamo SL and Bohor BF (1993a) Fingerprinting the K/T impact site and determining the time of impact by U–Pb dating of single shocked zircons from distal ejecta. *Earth and Planetary Science Letters* **119**, 425–9.
- Krogh TE, Kamo SL, Sharpton VL, Marin LE and Hildebrands AR (1993b) U–Pb ages of single shocked zircons linking distal K/T ejecta to the Chicxulub crater. *Nature* **366**, 731–4.
- Lawson DE (1972) Torridonian volcanic sediments. *Scottish Journal of Geology* **8**, 345–62.
- Lebeau LE and Ielpi A (2017) Fluvial channel-belts, floodbasins, and aeolian ergs in the Precambrian Meall Dearg Formation (Torridonian of Scotland): Inferring climate regimes from pre-vegetation clastic rock records. *Sedimentary Geology* **357**, 53–71.
- Leslie AG, Krabbendam M, Kimbell GS and Strachan RA (2010) Regional-scale lateral variation and linkage in ductile thrust architecture: the Oykel Transverse Zone, and mullions, in the Moine Nappe, NW Scotland. In *Continental Tectonics and Mountain Building: The Legacy of Peach and Horne* (eds RD Law, RWH Butler, RE Holdsworth, M Krabbendam and RA Strachan), pp. 359–81. Geological Society of London, Special Publication no. 335.
- Love GJ, Friend CRL and Kinny PD (2010) Palaeoproterozoic terrane assembly in the Lewisian Gneiss Complex on the Scottish mainland, south of Gruinard Bay: SHRIMP U–Pb zircon evidence. *Precambrian Research* **183**, 89–111.
- Ludwig KR (2012) *User's Manual for Isoplot 3.75: A geochronological toolkit for Microsoft Excel*. Berkeley Geochronological Center, Special Publication No. 5.
- MacDonald JM, Goodenough KM, Wheeler J, Crowley Q, Harley SL, Mariani E and Tatham D (2015) Temperature–time evolution of the Assynt Terrane of the Lewisian Gneiss Complex of Northwest Scotland from zircon U–Pb dating and Ti thermometry. *Precambrian Research* **260**, 55–75.
- Mark C, Cogné N and Chew DM (2016) Tracking exhumation and drainage divide migration of the Western Alps: A test of the apatite U–Pb thermochronometer as a detrital provenance tool. *Geological Society of America Bulletin* **128**, 1439–60.
- Mason AJ, Parrish RR and Brewer TS (2004) U–Pb geochronology of Lewisian orthogneisses in the Outer Hebrides, Scotland: implications for the tectonic setting and correlation of the South Harris Complex. *Journal of the Geological Society* **161**, 45–54.
- McGregor M, McFarlane CRM and Spray JG (2018) In situ LA-ICP-MS apatite and zircon U–Pb geochronology of the Nicholson Lake impact structure, Canada: Shock and related thermal effects. *Earth and Planetary Science Letters* **504**, 185–97.
- Moorbath S and Park RG (1972) The Lewisian chronology of the southern region of the Scottish mainland. *Scottish Journal of Geology* **8**, 51–74.
- Morgan J and Rebolledo-Vieyra M (2013) Geophysical studies of impact craters. In *Impact Cratering Processes and Products* (eds GR Osinski and E Pierazzo), pp. 211–22. Oxford, UK: Wiley-Blackwell.
- Morton AC and Hallsworth CR (1999) Processes controlling the composition of heavy mineral assemblages in sandstones. *Sedimentary Geology* **124**, 3–29.
- Moser DE (1997) Dating the shock wave and thermal imprint of the giant Vredefort impact, South Africa. *Geology* **25**, 7–10.
- Moser DE, Cupelli CL, Barker IR, Flowers RM, Bowman JR, Wooden J and Hart JR (2011) New zircon shock phenomena and their use for dating and reconstruction of large impact structures revealed by electron nanobeam (EBSD, CL, EDS) and isotopic U–Pb and (U–Th)/He analysis of the Vredefort dome. *Canadian Journal of Earth Sciences* **48**, 117–39.
- Nechaev VP and Ispording WC (1993) Heavy-mineral assemblages of continental margins as indicators of plate-tectonic environments. *Journal of Sedimentary Research* **63**, 1110–7.
- Nelson DR (2001) An assessment of the determination of depositional ages for Precambrian clastic sedimentary rocks by U–Pb dating of detrital zircons. *Sedimentary Geology* **141–142**, 37–60.
- O'Sullivan GJ, Chew DM, Morton AC, Mark C and Henrichs IA (2018) An integrated apatite geochronology and geochemistry tool for sedimentary provenance analysis. *Geochemistry, Geophysics, Geosystems* **19**, 1309–26.
- O'Sullivan GJ, Chew DM and Samson SD (2016) Detecting magma-poor orogens in the detrital record. *Geology* **44**, 871–4.
- Osinski GR, Preston L, Ferriere L, Prave T, Parnell J, Singleton A and Pickersgill AE (2011) The Stac Fada “impact ejecta” layer: not what it seems. *Meteoritics & Planetary Science* **46**, A181.
- Park RG, Tarney J and Connelly JN (2001) The Loch Maree Group: Palaeoproterozoic subduction–accretion complex in the Lewisian of NW Scotland. *Precambrian Research* **105**, 205–26.
- Parnell J, Mark D, Fallick AE, Boyce A and Thackrey S (2011) The age of the Mesoproterozoic Stoer Group sedimentary and impact deposits, NW Scotland. *Journal of the Geological Society* **168**, 349–58.
- Paton C, Hellstrom JC, Paul B, Woodhead JD and Hergt JM (2011) Iolite: Freeware for the visualisation and processing of mass spectrometric data. *Journal of Analytical Atomic Spectrometry* **26**, 2508–18.
- Paton C, Woodhead JD, Hellstrom JC, Hergt JM, Greig A and Maas R (2010) Improved laser ablation U–Pb zircon geochronology through robust down-hole fractionation correction. *Geochemistry, Geophysics, Geosystems* **11**, Q0AA06.
- Petrus JA and Kamber BS (2012) VizualAge: A novel approach to laser ablation ICP-MS U–Pb geochronology data reduction. *Geostandards and Geoanalytical Research* **36**, 247–70.
- Piccoli PM and Candela PA (2002) Apatite in igneous systems. *Reviews in Mineralogy and Geochemistry* **48**, 255–92.
- Rainbird RH, Hamilton MA and Young GM (2001) Detrital zircon geochronology and provenance of the Torridonian, NW Scotland. *Journal of the Geological Society* **158**, 15–27.
- Reddy SM, Johnson TE, Fischer S, Rickard WDA and Taylor RJM (2015) Precambrian reidite discovered in shocked zircon from the Stac Fada impactite, Scotland. *Geology* **43**, 899–902.
- Rodrigues B, Chew DM, Jorge RCGS, Fernandes P, Veiga-Pires C and Oliveira JT (2015) Detrital zircon geochronology of the Carboniferous Baixo Alentejo Flysch Group (South Portugal); constraints on the provenance and geodynamic evolution of the South Portuguese Zone. *Journal of the Geological Society* **172**, 294–308.
- Sanders IS and Johnston JD (1989) The Torridonian Stac Fada Member: an extrusion of fluidised peperite? *Transactions of the Royal Society of Edinburgh: Earth Sciences* **80**, 1–4.
- Sanders IS, Van Calsteren PWC and Hawkesworth CJ (1984) A Grenville Sm–Nd age for the Glenelg eclogite in north-west Scotland. *Nature* **312**, 439.
- Schoene B and Bowring S (2006) U–Pb systematics of the McClure Mountain syenite: thermochronological constraints on the age of the 40Ar/39Ar standard MMhb. *Contributions to Mineralogy and Petrology* **151**, 615–30.
- Simms MJ (2015) The Stac Fada impact ejecta deposit and the Lairg Gravity Low: evidence for a buried Precambrian impact crater in Scotland? *Proceedings of the Geologists' Association* **126**, 742–61.

- Sircombe KN and Freeman MJ (1999)** Provenance of detrital zircons on the Western Australia coastline—Implications for the geologic history of the Perth basin and denudation of the Yilgarn craton. *Geology* **27**, 879–82.
- Spear FS and Pyle JM (2002)** Apatite, monazite, and xenotime in metamorphic rocks. *Reviews in Mineralogy and Geochemistry* **48**, 293–335.
- Stacey JS and Kramers JD (1975)** Approximation of terrestrial lead isotope evolution by a two-stage model. *Earth and Planetary Science Letters* **26**, 207–21.
- Stewart AD (1982)** Late Proterozoic rifting in NW Scotland: the genesis of the ‘Torridonian’. *Journal of the Geological Society* **139**, 413–20.
- Stewart AD (1990)** Geochemistry, provenance and climate of the Upper Proterozoic Stoer Group in Scotland. *Scottish Journal of Geology* **26**, 89–97.
- Stewart AD (2002)** The later Proterozoic Torridonian rocks of Scotland: their sedimentology, geochemistry and origin. *Geological Society of London, Memoir* **24**, 130.
- Sylvester PJ, Crowley JL and Schmitz MD (2013)** U/Pb zircon age of Mistastin Lake crater, Labrador, Canada - implications for high-precision dating of small impact melt sheets and the end Eocene extinction. *Mineralogical Magazine* **77**, 2295.
- Thackrey S, Walkden G, Indares A, Horstwood M, Kelley S and Parrish R (2009)** The use of heavy mineral correlation for determining the source of impact ejecta: A Manicouagan distal ejecta case study. *Earth and Planetary Science Letters* **285**, 163–72.
- Thomas WA (2011)** Detrital-zircon geochronology and sedimentary provenance. *Lithosphere* **3**, 304–8.
- Thomson SN, Gehrels GE, Ruiz J and Buchwaldt R (2012)** Routine low-damage apatite U-Pb dating using laser ablation–multicollector–ICPMS. *Geochemistry, Geophysics, Geosystems*, **13**, Q0AA21.
- Upton B, Emeleus CH, Heaman LM, Goodenough KM and Finch AA (2003)** Magmatism of the mid-Proterozoic Gardar Province, South Greenland: chronology, petrogenesis and geological setting. *Lithos* **68**, 43–65.
- Van de Kamp PC and Leake BE (1997)** Mineralogy, geochemistry, provenance and sodium metasomatism of Torridonian rift basin clastic rocks, NW Scotland. *Scottish Journal of Geology* **33**, 105–24.
- Vermeesch P (2004)** How many grains are needed for a provenance study? *Earth and Planetary Science Letters* **224**, 441–51.
- Vermeesch P (2012)** On the visualisation of detrital age distributions. *Chemical Geology* **312–313**, 190–4.
- Vermeesch P (2013)** Multi-sample comparison of detrital age distributions. *Chemical Geology* **341**, 140–6.
- Walkden G, Parker J and Kelley S (2002)** A late Triassic impact Ejecta layer in Southwestern Britain. *Science* **298**, 2185–8.
- Waters FG, Cohen AS, O’Nions RK and O’Hara MJ (1990)** Development of Archaean lithosphere deduced from chronology and isotope chemistry of Scourie Dykes. *Earth and Planetary Science Letters* **97**, 241–55.
- Went DJ (2005)** Pre-vegetation alluvial fan facies and processes: an example from the Cambro-Ordovician Rozel Conglomerate Formation, Jersey, Channel Islands. *Sedimentology* **52**, 693–713.
- White LF, Darling JR, Moser DE, Reinhard DA, Prosa TJ, Bullen D, Olson D, Larson DJ, Lawrence D and Martin I (2017)** Atomic-scale age resolution of planetary events. *Nature Communications* **8**, 15597.
- Whitehouse MJ and Bridgwater D (2001)** Geochronological constraints on Paleoproterozoic crustal evolution and regional correlations of the northern Outer Hebridean Lewisian complex, Scotland. *Precambrian Research* **105**, 227–45.
- Whitehouse MJ, Claesson S, Sunde T and Vestin J (1997)** Ion microprobe U-Pb zircon geochronology and correlation of Archaean gneisses from the Lewisian Complex of Gruinard Bay, northwestern Scotland. *Geochimica et Cosmochimica Acta* **61**, 4429–38.
- Whitehouse MJ and Kemp AIS (2010)** On the difficulty of assigning crustal residence, magmatic protolith and metamorphic ages to Lewisian granulites: constraints from combined in situ U–Pb and Lu–Hf isotopes. In *Continental Tectonics and Mountain Building: The Legacy of Peach and Horne* (eds RD Law, RWH Butler, RE Holdsworth, M Krabbendam and RA Strachan), pp. 81–101. Geological Society of London, Special Publication no. 335.
- Wiedenbeck M, Allé P, Corfu F, Griffin WL, Meier M, Oberli F, Quadt AV, Roddick JC and Spiegel W (1995)** Three natural zircon standards for U–Th–Pb, Lu–Hf, trace element and REE analyses. *Geostandards Newsletter* **19**, 1–23.
- Young GM (2002)** Stratigraphy and geochemistry of volcanic mass flows in the Stac Fada Member of the Stoer Group, Torridonian, NW Scotland. *Earth and Environmental Science Transactions of the Royal Society of Edinburgh* **93**, 1–16.
- Zattin M, Andreucci B, Thomson SN, Reiners PW and Talarico FM (2012)** New constraints on the provenance of the ANDRILL AND-2A succession (western Ross Sea, Antarctica) from apatite triple dating. *Geochemistry, Geophysics, Geosystems* **13**, Q10016.
- Zhu ZK, O’Nions RK, Belshaw NS and Gibb AJ (1997)** Lewisian crustal history from in situ SIMS mineral chronometry and related metamorphic textures. *Chemical Geology* **136**, 205–18.